Micro-optics

Photoswitchable Microlens Arrays**

*Jongseong Kim, Michael J. Serpe, and L. Andrew Lyon**

Micro-optical structures have been of recent interest to both industrial and academic pursuits with regards to the miniaturization of optical elements and the development of novel functional materials.[1–3] Microlens array technology has also been used recently as a route to highly parallel image projection to enable microlens-directed photolithography.[4,5] While microlens array technology is constantly being improved with respect to fabrication methods and optical quality, these arrays are typically comprised of optical elements with fixed focal lengths, relatively large diameters, and/or slow focal length switching speeds. Furthermore, many array technologies require meticulous photolithographic processing for fabrication.[6–9] It would be a major advancement if an array of micron-scale optical elements with dynamically tunable focal lengths could be prepared in a facile, inexpensive, and scalable fashion. Another challenge is to construct true microlens arrays for which the focal length of individual lens elements can be addressed on demand and independently of other array elements. Accomplishment of the above goals would represent an enabling technology for a new class of applications in foveated vision, parallel chemical sensing, and beam steering, as well as an expansion of the tools available to current efforts in the field.

We have previously shown by using an electrostatic self-assembly approach that ordered microlens arrays could be fabricated on glass substrates and that they effectively function as optical elements that are capable of focusing images in air and water.[10,11] The lensing ability is mainly a result of the hemispherical shape of the particle that results from its immobilization on the solid support and the contrast in the refractive index (RI) between the deswollen microgel polymer (≈ 1.4) and the medium. Tunability of the focal length in a microlens array in water has also been demonstrated from the thermoresponsivity of pNIPAm-co-AAc (pNIPAm = poly(*N*-isopropylacrylamide), AAc = acrylic acid) microgels in aqueous solution. As the temperature of a pNIPAm microgel in solution is increased to the intrinsic lower critical solution temperature (LCST) of the polymer, the microgels undergo a phase transition from a solvent-swollen state to a deswollen state.[12,13] Accordingly, the thermoresponsive optical properties of the microlens arrays can be understood not only by considering the microgels to be more optically dense above the LCST but also by considering that lensing power is dependent upon the ratio of the RI of the lens material and the surrounding medium, such that a higher difference in the RI results in a shorter focal length lens.

Here we describe the first demonstration of microlens arrays comprised of fast-responding, reversible, phototunable lens elements, which are prepared using simple wet-chemical methods. These arrays are fabricated by exposing 3-aminopropyltrimethoxysilane (APTMS)-functionalized glass substrates to citrate-stabilized Au nanoparticles (16 ± 1.6 nm), which attach themselves to the glass substrate through electrostatic interactions.[14] The presence of Au nanoparticles on the surface allows for local heating of the sample through excitation of surface plasmon modes on the Au nanoparticles with a frequency-doubled Nd:YAG laser ($\lambda = 532$ nm).[15] Plasmon excitation results in a transfer of energy to the environment in the form of thermal dissipation through electron–phonon and phonon–phonon coupling interactions.[16] Note that other means of heating the particles, such as by temperature-jump dyes and IR irradiation, have also been reported.[17,18] This Au nanoparticle-coated substrate is subsequently rendered positively charged by exposure to the cationic polyelectrolyte poly(allylamine hydrochloride) (PAH). PNIPAm-co-AAc microgels are attached to the substrate by adding a drop of an aqueous solution of the microgel (10% v/v) at pH 6.5 to the APTMS–Au–PAH-modified glass substrate. In this fashion, the microgel particles coat the nanoparticle-modified glass substrate by electrostatic self-assembly. At this pH value, the microgels are anionic, which allows good adhesion to the cationic substrate. After the substrate is dried for 24 hours, it is immersed in and rinsed with deionized water to leave behind only the microgels strongly attached to the substrate through electrostatic interactions. Figure 1 shows a schematic depiction and a scanning electron microscopy (SEM) image of this structure.

For lens-tuning studies, the microlens array was then exposed to solutions at various pH values by introduction of the appropriate solution into the void space of a microlens array/silicone gasket/coverslip sandwich assembly. The temperature of this sample was controlled by a Peltier heating/cooling stage mounted on the sample holder of an optical microscope. Optical microscopy measurements were performed on this assembly to explore the phototuning of the microlens array in response to laser excitation. An Olympus IX-70 inverted optical microscope equipped with a 1.30 N.A. (N.A. = numerical aperture) oil-immersion 100× objective, a microscope objective heater, a Peltier-based temperature stage with an integrated thermocouple, and a black and white CCD camera (PixelFly, Cooke Corporation) was used for imaging the pattern under continuous-wave laser irradiation, and an Itronx Imaging Technologies FASTCAM DVR CCD camera was used to image the lenses exposed to pulsed laser excitation. In this arrangement, we take advantage of the conjugate focal planes in the microscope by placing a pattern near a plane conjugate to the back focal plane of the objective. When the microgels act as lens elements, they

[*] J. Kim, Dr. M. J. Serpe, Prof. L. A. Lyon
School of Chemistry and Biochemistry
Georgia Institute of Technology
Atlanta, GA 30332-0400 (USA)
Fax: (+1) 404-894-7452
E-mail: lyon@chemistry.gatech.edu

[**] L.A.L. acknowledges support from a Sloan Fellowship and a Camille Dreyfus Teacher–Scholar Award. We thank Prof. M. Srinivasarao for the fast frame rate CCD camera used in this study.

Supporting information for this article is available on the WWW under http://www.angewandte.org or from the author.

 DOI: 10.1002/ange.200461538

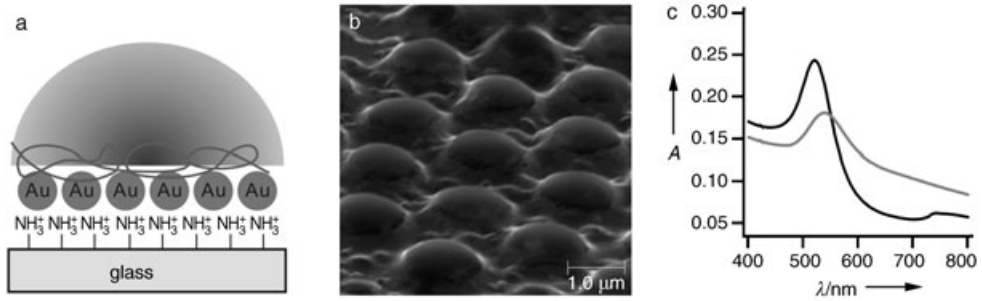

Figure 1. a) Depiction of the multicomponent film used to create photoswitchable microlens arrays. b) SEM image of the constructed microlens array at grazing angle. c) UV/Vis spectra of Au nanoparticles in solution (black) and bound to substrate (gray).

change the effective focal length of the microscope, bringing the back focal plane of the objective near the eyepoint. This is observed as a projection of the pattern through each active element in the lens array. A diagram of the microscopy setup is shown in Scheme 1.

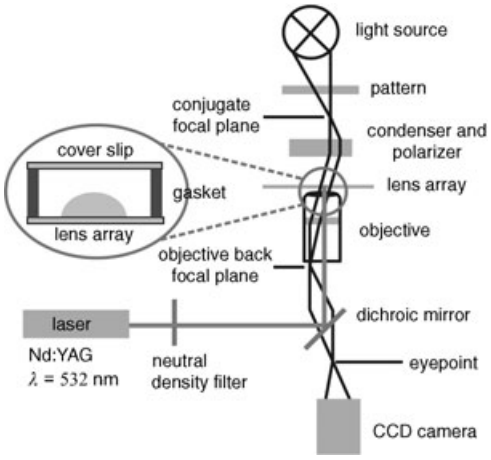

Scheme 1. Inverted light microscopy setup used for detection of the photoswichable behavior of microlens arrays in the liquid phase. The lenses at the imaging plane move the objective back focal plane to the eyepoint, thus bringing a pattern placed near the source into focus.

The key characteristics of the phototuning of this construction relate to the optical properties of the colloidal Au array and the thermoresponsivity of the microgel lens elements. UV/Vis spectroscopy was used to confirm the presence of Au nanoparticles on the glass substrate following assembly. Figure 1c shows the spectra of Au nanoparticles either in aqueous solution or on a substrate coated with a microlens array. The absorption spectrum of the substrate-bound Au nanoparticles is shifted to slightly higher wavelengths than that of the free Au nanoparticles in solution. A long-wavelength shoulder is also apparent in the spectrum of the lens array and is most likely caused by some aggregation of Au nanoparticles on the substrate during assembly, while the shift in the plasmon resonance results from the microlens array. The deswollen microlenses present a higher local refractive index to the surface of the Au nanoparticles, thereby shifting the plasmon resonance to lower energy.

The photoresponsivity of the microlens arrays was initially investigated by monitoring the projection of a triangle pattern through the lenses while they were exposed to a solution at pH 3.0 in response to various laser powers and bath temperatures. Figure 2a and b show the focal length tunability of the

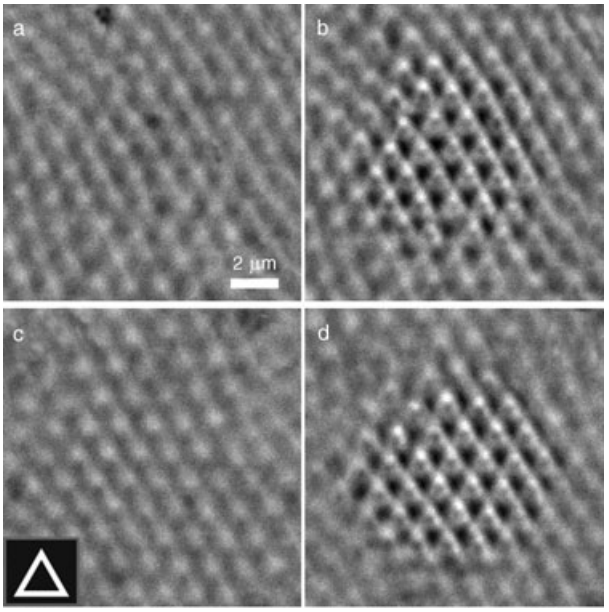

Figure 2. Photoswitching of microlens arrays as a function of laser power and solution temperature at pH 3.0. Arrays at 25 °C (a and b) and 10 °C (c and d) show laser-power-dependent optical properties by projecting a triangle pattern (c, lower left corner) only when the laser power is sufficient to produce the necessary temperature jump to above the microgel LCST. Laser powers: 10.22 mW μm^{-2} (a), 38.45 mW μm^{-2} (b, c), and 88.90 mW μm^{-2} (d). It can also be seen that each lens is capable of projecting an image only in the region surrounding the incident laser light excitation.

microlens arrays at a bath temperature of 25 °C upon laser exposure. Each lens projects the triangle image only in the region of laser light excitation, where the effective temperature is higher than the lower critical solution temperature of the microgel. The number of lenses that display a high quality image is also tunable by varying the laser power (see Supporting Information). Similarly, Figure 2c and d show the focal length tunability of the microlens arrays at a bath temperature of 10 °C upon laser exposure. A smaller area of

the array is switched under these conditions, as the bath temperature is further from the LCST of pNIPAm (31 °C). Note that the same laser power is impingent on the array in Figure 2 b and c. As a fixed laser power induces a fixed jump in temperature, decreasing the temperature of the bath to far below the LCST results in a photoinduced temperature excursion that is now below the LCST of the polymer (Figure 2 c). It is also theoretically possible to control single lens elements of the array by this method. As the laser spot is essentially diffraction-limited in size (≈266 nm in diameter) under these illumination conditions, it is in fact smaller than an individual lens. By controlling the bath temperature and the laser intensity, one can therefore interrogate a single lens element (see Supporting Information).

Figure 3 a and b show images projected through the microlens array at 25 °C at pH 6.5 as a function of laser power. A comparison of Figure 2 b and Figure 3 a, for which the laser powers are identical, suggests that the microlens array at pH 6.5 is less sensitive to laser irradiation than at pH 3.0. This behavior is a result of the higher LCST of the microgels at this pH, caused by deprotonation of AAc within the microgel network at pH values greater than the pK_a value (p$K_a \approx$ 4.25).[19] As expected, the lensing ability of the microlens is unaffected by temperature up to the transition temperature of approximately 48 °C, as observed by the bulk heating experiments (see Supporting Information). Figure 3 b and d illustrate that the microlens array is again extremely sensitive to the bath temperature, as indicated by a decrease in the area of the modulated region at low temperature. This effect can also be confirmed by comparing the modulated area in Figure 2 d to Figure 3 d and is caused by the lower LCST of the microgels at pH 3.0, therefore they are able to respond to smaller jumps in temperature than the microgels at pH 6.5.

The reversibility and response rate of the microlens array are shown in Figure 4. The laser modulation frequency was controlled by passing it through an optical chopper. Figure 4 row a shows that the optical properties of the microlens array can be fully modulated in a completely reversible fashion by using laser pulses of 10 ms. This experiment was performed without the projection of a pattern through the array as the camera was not sensitive enough to detect the projected image while acquiring images at 2000 fps (frames per second).

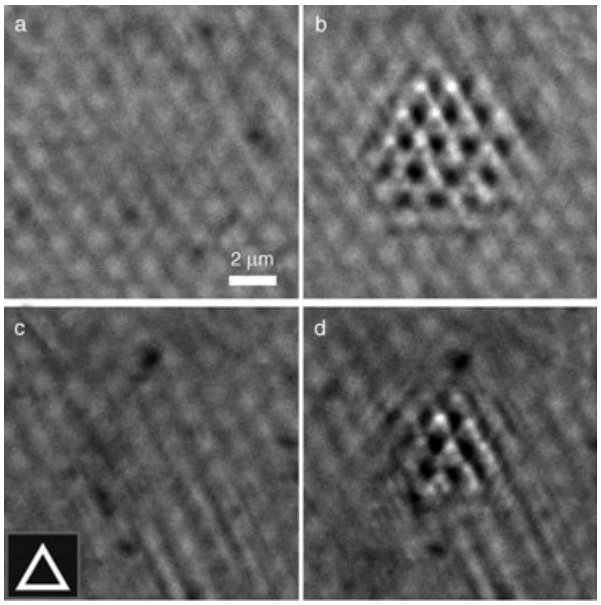

Figure 3. Photoswitching of microlens arrays as a function of laser power and solution temperature at pH 6.5. Again it can be seen that the arrays at 25 °C (a and b) and 10 °C (c and d) show laser-power-dependent optical properties by projecting a triangle pattern (c, lower left corner) only when the laser power is sufficient to produce the necessary temperature jump to above the microgel LCST. Laser powers: 38.45 mW μm^{-2} (a), 88.90 mW μm^{-2} (b, d), and 48.56 mW μm^{-2} (c). By comparison to Figure 2 it can be seen that more laser power is required to modulate the micro-optical array at this pH value.

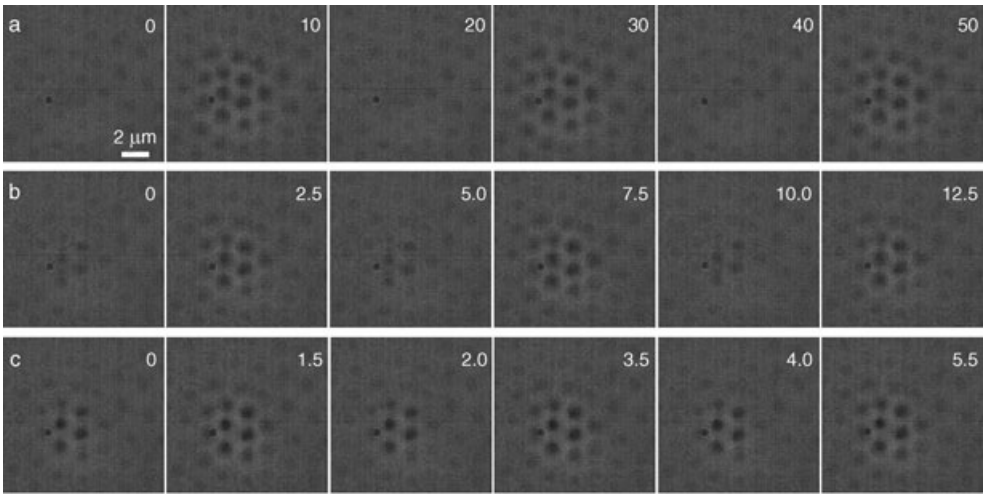

Figure 4. Images captured with a fastcam DVR CCD camera at 2000 fps while chopping the Nd:YAG laser source at 50 Hz (a), 200 Hz (b), and 500 Hz (c) in solution at pH 6.5 and at 15 °C. The optical properties of the array can be reversibly modulated in phase with laser pulses of 50 Hz (a). However, once the laser modulation frequency exceeds the rate of thermal diffusion from the microgels, the modulation of the microlens array diminishes (b and c). The laser intensity at the array surface is 184.97 mW μm^{-2}. The numbers in the upper-right corners of each image indicate the time interval Δt in milliseconds after which the image was recorded.

The apparent response time of microlenses in the array was measured at $< 500\,\mu s$ as we cannot resolve intermediate stages of microgel deswelling at 2000 fps under the conditions presented in Figure 4 (see Supporting Information). In other words, individual lens elements go from a non-lensing to a lensing state within one frame at this image-capture rate. Literature reports place microgel deswelling rates on the timescale of tens to hundreds of microseconds, depending on the network density and particle size.[18] Figure 4b and c also show that this reversibility is diminished upon increasing the laser repetition frequency from 200 to 500 Hz because, while microgel deswelling is caused by fast thermal dissipation from the laser-excited Au nanoparticles to the microlenses, the reswelling of the microgel is limited by the slow dissipation of heat away from the substrate. Thus, the microlens array appears totally deswollen at 500 Hz as the pulsing frequency is faster than the microgel reswelling rate.

In conclusion, by using simple wet-chemical methods we have fabricated a high-density microlens array that can be tuned or switched by an external laser source. The fabrication technology is inexpensive, scalable, and rapid, in contrast to traditional micromolding or photolithographic approaches. The unique characteristics of the micro-optics include the ability to confine the tunable region to the single-microlens scale, fast response rate ($\approx$10-fold faster than video rate), and highly reversible behavior under pulsed laser control. These characteristics make this system an attractive enabling technology for the future development of agile micro-optical components.

Received: August 4, 2004
Revised: November 1, 2004
Published online: January 20, 2005

Keywords: gels · gold · laser spectroscopy · nanotechnology · surface plasmon resonance

[1] Y. N. Xia, G. M. Whitesides, *Angew. Chem.* **1998**, *110*, 568; *Angew. Chem. Int. Ed.* **1998**, *37*, 551.
[2] P. D. Yang, G. Wirnsberger, H. C. Huang, S. R. Cordero, M. D. McGehee, B. Scott, T. Deng, G. M. Whitesides, B. F. Chmelka, S. K. Buratto, G. D. Stucky, *Science* **2000**, *287*, 465.
[3] M. H. Qi, E. Lidorikis, P. T. Rakich, S. G. Johnson, J. D. Joannopoulos, E. P. Ippen, H. I. Smith, *Nature* **2004**, *429*, 538.
[4] H. K. Wu, T. W. Odom, G. M. Whitesides, *J. Am. Chem. Soc.* **2002**, *124*, 7288.
[5] M. H. Wu, G. M. Whitesides, *Adv. Mater.* **2002**, *14*, 1502.
[6] Y. N. Xia, E. Kim, X. M. Zhao, J. A. Rogers, M. Prentiss, G. M. Whitesides, *Science* **1996**, *273*, 347.
[7] Y. Lu, Y. D. Yin, Y. N. Xia, *Adv. Mater.* **2001**, *13*, 34.
[8] S. Yang, T. N. Krupenkin, P. Mach, E. A. Chandross, *Adv. Mater.* **2003**, *15*, 940.
[9] H. W. Ren, Y. H. Fan, S. Gauza, S. T. Wu, *Opt. Commun.* **2004**, *230*, 267.
[10] M. J. Serpe, J. Kim, L. A. Lyon, *Adv. Mater.* **2004**, *16*, 184.
[11] J. Kim, M. J. Serpe, L. A. Lyon, *J. Am. Chem. Soc.* **2004**, *126*, 9512.
[12] D. Gan, L. A. Lyon, *J. Am. Chem. Soc.* **2001**, *123*, 7511.
[13] C. D. Jones, L. A. Lyon, *Macromolecules* **2003**, *36*, 1988.
[14] R. G. Freeman, K. C. Grabar, K. J. Allison, R. M. Bright, J. A. Davis, A. P. Guthrie, M. B. Hommer, M. A. Jackson, P. C. Smith, D. G. Walter, M. J. Natan, *Science* **1995**, *267*, 1629.
[15] C. D. Jones, M. J. Serpe, L. Schroeder, L. A. Lyon, *J. Am. Chem. Soc.* **2003**, *125*, 5292.
[16] S. Link, M. A. El-Sayed, *Int. Rev. Phys. Chem.* **2000**, *19*, 409.
[17] S. Nayak, L. A. Lyon, *Chem. Mater.* **2004**, *16*, 2623.
[18] J. Wang, D. Gan, L. A. Lyon, M. A. El-Sayed, *J. Am. Chem. Soc.* **2001**, *123*, 11284.
[19] C. D. Jones, L. A. Lyon, *Macromolecules* **2000**, *33*, 8301.

